Cortical amyloid burden and age moderate hippocampal activity in cognitively-normal adults

Zhuang Song[a,*], Ian M. McDonough[a], Peiying Liu[b], Hanzhang Lu[b], Denise C. Park[a]

[a]Center for Vital Longevity, University of Texas at Dallas, Dallas, TX 75235, USA
[b]Department of Radiology & Radiological Science, Johns Hopkins University, MD 21287, USA

ARTICLE INFO

ABSTRACT

Neurodegeneration in the medial temporal lobe, particularly in the hippocampus, is viewed as the primary source of AD-related memory deficits. Yet, in the earliest preclinical phase of Alzheimer's disease (AD), amyloid-beta (Aβ) plaques deposit primarily in the neocortex, not in the medial temporal lobe. Tau tangles, however, do often aggregate in the medial temporal lobe in parallel with amyloid deposition in the neocortex in AD. In the present study, we focused on the relationship between cortical amyloid deposition and hippocampal activity during a memory-encoding task in a sample of cognitively-normal elderly aged 60–89. We hypothesized that age would moderate the Aβ effect on hippocampal activity, and could explain some of the mixed findings in the literature. We report that high cortical Aβ load was associated with lower task-related hippocampal activity during memory encoding. Importantly, this relationship was found more evident in the younger elderly, even after controlling for subsequent recognition memory of the in-scanner task and a general episodic memory construct score. Furthermore, regional cerebrovascular reactivity measured in a subset of participants showed little role in modifying the age-dependent Aβ effect on hippocampal activity. Our findings support the idea that age is an important variable in understanding hippocampal function in preclinical AD.

1. Introduction

The medial temporal lobe (MTL) is particularly vulnerable to Alzheimer's disease (AD) (Braak and Braak 1991). Postmortem as well as recent imaging studies of brain amyloid-beta (Aβ) deposition have led to the recognition that there is a decades-long incubation period of AD (Jack and Holtzman 2013). During this period of time, pathology starts to develop in the absence of cognitive symptoms, the so-called preclinical phase of AD (Sperling et al. 2011). Aβ plaques tend to deposit in the neocortex and this deposition is highly correlated with tau tangle aggregation in the MTL (Braak et al. 2011; Sperling et al. 2014). Despite growing knowledge about the distribution and spread of amyloid plaques and tau tangles, little is known about how neural activity in MTL is altered by the early pathological development of AD, particularly in the hippocampus.

Although there have been several investigations of the effect of amyloid deposition on neural activity in the MTL, the existing data have failed to yield a clear picture of the relationship. A recent prospective study found that the cognitively-normal elderly who progressed to AD had lower baseline metabolism, based on cerebral blood volume, in the entorhinal cortex than those who didn't progress (Khan et al. 2014). Blood-oxygen-level dependent (BOLD) functional MRI (fMRI) studies of hippocampal activation in cognitively-normal adults, however, have yielded mixed results regarding the association of cortical Aβ burden with hippocampal activity. For example, Mormino et al. (2012) reported that high cortical Aβ deposition was related to higher task-related hippocampal activity in successful memory encoding, while other studies did not find such a relationship (Sperling et al. 2009; Elman et al. 2014; Huijbers et al. 2014; Kennedy et al., 2012). We note, however, that while Huijbers et al. (2014) did not observe such a relationship in the hippocampus, they did find a relationship in the entorhinal cortex.

The mixed findings regarding the Aβ effect on task-related hippocampal activity may have occurred for several reasons. First the effect of age has not been systematically investigated in previous studies. Increasing evidence reveals that task-related hippocampal activity may be reduced with age (Persson et al. 2012). Therefore it may be the case that the younger-old are more likely to show the Aβ effect while the older-old do not, such that the inclusion of the older old adults in the study sample might result in a "washing out" of the Aβ effect on hippocampal activity. Although previous studies often controlled age as a nuisance variable in analysis, it might have been beneficial to

* Corresponding author.
E-mail address: zhuang.song@utdallas.edu (Z. Song).

analyze the interaction between age and Aβ in these studies. Second, task-related hippocampal activity is often subtle with a small percentage signal change (Stark and Squire 2001). The small range of task-related fMRI activity in the hippocampus makes it difficult to detect the Aβ effect in this region compared to other brain regions. Third, differences in neurovascular coupling may alter fMRI signals in the brain with age as well as with a variety of diseases, but few studies have examined or controlled for this important factor (D'Esposito et al. 2003; Liu et al. 2013).

In the present study, we attempted to address these possible explanations. We collected BOLD-fMRI data during an incidental memory-encoding task, in conjunction with positron emission tomography (PET) to measure Aβ plaques using F18-AV-45 florbetapir radiotracer. We then examined the effect of cortical amyloid load and its interaction with age on task-related hippocampal activity, using both regions of interest (ROI)-based as well as exploratory voxelwise approaches. In addition, a subset of participants had cerebrovascular reactivity (CVR) measured with hypercapnia MRI, allowing us to assess the impact of CVR on task-related fMRI activity.

2. Methods and materials

2.1. Participants

Our sample consisted of 82 cognitively-normal elderly participants (aged 60–89 years) in the Dallas Lifespan Brain Study (DLBS) who underwent a cognitive battery, Aβ-PET, and fMRI, after excluding 5 participants for severe head motion during fMRI scanning. DLBS participants were recruited from the community and screened against major heart and brain diseases. All participants were right-handed, native English speakers with a Mini Mental State Examination (MMSE) score of 26 or greater. Informed consent for the study was collected in accordance with the policy of the Institutional Review Board of the University of Texas Southwestern Medical Center and the University of Texas at Dallas. Demographic information for all participants is presented in Table 1.

Table 1
Demographic characteristics and cognitive performance of the Low and High Aβ status groups.

	Aβ-Low	Aβ-High
N	52	30
Age	72.6 (7.9)	76.8 (8.4)
Age range	61 ~ 88	60 ~ 89
Sex (F/M)	30/22	17/13
Education (Y)	16.2 (2.5)	15.8 (2.6)
ApoE4 allele (N/%)	5/9.6%	8/26.7%
SUVr	1.12 (0.05)	1.39 (0.19)
SUVr range	0.95 ~ 1.19	1.20 ~ 1.78
MMSE range	26 ~ 30	26 ~ 30
Subsequent recognition hit rate	0.74 (0.12)	0.74 (0.15)
Subsequent recognition false alarm rate	0.53 (0.16)	0.57 (0.20)
Subsequent recognition accuracy	0.60 (0.06)	0.59 (0.05)
Episodic memory (Z-score)	0.08 (0.79)	−0.14 (0.86)
Processing speed (Z-score)	0.20 (0.86)	−0.34 (0.92)*
Working memory (Z-Score)	0.12 (0.83)	−0.20 (0.85)
Fluid reasoning (Z-score)	0.09 (0.88)	−0.16 (0.86)
Crystallized intelligence (Z-score)	0.09 (0.94)	−0.15 (0.93)
Hypercapnia MRI (N)	34	16

Note: Means and SDs are reported for continuous variables. The subsequent recognition memory scores were derived from the fMRI task. The cognitive construct scores, including episodic memory, were derived from a cognitive test battery. The asterisk symbol indicates significant difference between the two groups in simple t-tests that were conducted for measures of subsequent recognition memory and cognitive scores (i.e. $p < 0.05$). SUVr, standard uptake value ratio; MMSE, mini mental state exam.

2.2. Behavioral measures outside the scanner

The cognitive battery, completed by all participants, was used to create five cognitive constructs. All constructs were created by calculating Z-scores for each measure associated with a given construct across all participants included in the final sample and averaging them together (see Table 1). The primary construct of interest was episodic memory which was formed from three measures: the number of correct items recalled on the immediate and delayed Hopkins Verbal Leaning Task (Brandt 1991) and the number of correct items recognized on the Verbal Recognition Memory task from the Cambridge Neuropsychological Test Automated Battery (CANTAB) (Robbins et al. 1994), Cronbach $\alpha = 0.76$. The processing speed construct included the number of correct items on the Digit Symbol task (Wechsler 1997) and the Digit Comparison task (Salthouse and Babcock 1991), Cronbach $\alpha = 0.80$. Working memory was measured using the number of correct items on the Letter-Number Sequencing task (Wechsler 1997) and the sum of the perfectly-recalled trials on the Operation Span task (Turner and Engle 1989), Cronbach $\alpha = 0.53$. Fluid reasoning was measured using the total score on the ETS Letter Sets task (Ekstrom et al. 1976) and accuracy on the Raven's Progressive Matrices task (Raven et al. 1998), Cronbach $\alpha = 0.73$. Crystallized intelligence was measured using the total number of correct items on the ETS Advanced Vocabulary Scale (Ekstrom et al. 1976) and Shipley Vocabulary Scale (Zachary 1986), Cronbach $\alpha = 0.87$.

2.3. PET image acquisition and analysis

The PET scan was performed on a Siemens ECAT HR PET scanner. Participants were injected with a 370 MBq (10 mCi) bolus of F18-AV-45 florbetapir radiotracer. At 30 min post injection participants were positioned on the imaging table of the scanner. Soft Velcro straps and foam wedges were used to secure the participant's head, which was positioned with laser guides. A 2-frame by 5 min each dynamic emission was acquired 50 min after the injection of the florbetapir radiotracer, immediately after 7 min scan of internal rod source transmission. The transmission images were reconstructed using back-projection and a 6 mm FWHM Gaussian filter. Each participant's PET scan was spatially normalized to a Florbetapir template ($2 \times 2 \times 2$ mm^3 voxels) in the MNI template space. A standardized uptake value ratio (SUVr) for each subject was defined as the ratio of mean Aβ tracer uptake within 8 predefined cortical gray matter regions relative to cerebellar gray matter. The 8 cortical regions were dorsal lateral prefrontal cortex, orbitofrontal cortex, lateral parietal cortex, posterior cingulate cortex, anterior cingulate cortex, precuneus, lateral temporal cortex, and occipital lobe.

2.4. MRI acquisition

MRI data were acquired in a Philips Achieva 3 T MR scanner (Philips Medical Systems, Best, The Netherlands) equipped with an 8-channel head-coil. T1-weighted 3D high-resolution anatomical images were acquired with MP-RAGE pulse sequence (FOV = 25×256 mm^2, matrix size 256×256, TR = 8.18 ms, TE = 3.76 ms, flip angle 12°, voxel size $1 \times 1 \times 1$ mm^3, 160 sagittal slices). FMRI was acquired with whole brain T2*-weighted interleaved echo-planar images (EPIs) (SENSE = 2, FOV = 220×220 mm^2, matrix size 64×64, TR = 2000 ms, TE = 25 ms, flip angle 80°, voxel size $3.4 \times 3.4 \times 3.5$ mm^3, 43 axial slices oriented parallel to the AC-PC line). FMRI data were acquired during the study phase in 3 runs. Each run was 5.7 min long and comprised of 171 volumes. Five dummy volumes were collected at the beginning of each run but discarded to allow for T1 stabilization.

2.5. Hypercapnia procedures

A subset of the participants had CVR measured with hypercapnia MRI (N = 50, Table 1). Participants inhaled 5% CO_2 gas when BOLD-fMRI was simultaneously acquired with identical imaging parameters to the task fMRI described above. The CVR measurement protocol was described in detail previously (Lu et al. 2014). Briefly, during the hypercapnia MRI scan, participants breathed room air and the prepared gas in an interleaved fashion switching every 1 min. The prepared gas was a mixture of 5% CO_2, 74% N_2 and 21% O_2. The end-tidal CO_2 (EtCO$_2$), the CO_2 concentration in the lungs and thus arterial blood, was also recorded throughout the breathing task using a capnograph device (Capnogard, model 1265, Novametrix Medical Systems, CT). The total duration for the hypercapnia MRI scan was 7 min.

2.6. fMRI task

All participants received an incidental memory-encoding task during an event-related fMRI scan (Gutchess et al. 2005). During each experimental trial, participants viewed a picture of an outdoor scene for 3 s and indicated whether the picture contained water by pressing a button with the right hand. Half of the pictures contained water in the scene and half did not. At the end of each trial, a fixation cross was presented and stayed on the screen until the next trial began. The interval between experimental trials varied between 4 s and 14 s. The encoding list was comprised of a random ordering of 96 pictures of outdoor scenes in three runs (32 pictures each run). A surprise recognition test was administered outside of the scanner approximately 20 min after the end of the study phase. The recognition test list included the 96 studied pictures and 96 new pictures (lures), which were counterbalanced across participants. Each of the lures was matched in content to one of the study pictures. For example if a study picture contained an image of a lake surrounded by a forest, a lure would be included of a different picture that had similar content of a lake surrounded by a forest. The purpose of this content matching was to make the picture recognition task sufficiently difficult that ceiling performance, which is characteristic of picture recognition tasks, would be avoided. Participants were instructed to indicate whether they remembered each picture by making one of three judgments: high confidence that the picture was presented at study; low confidence that the picture was presented at study; or new picture. The subsequent recognition test was self-paced with a maximum of 4 s for each trial. The accuracy of subsequent recognition memory was defined as the percentage of items either correctly recognized if they were presented during the study session (Hit) or correctly rejected if they were not presented during the study session (Correct Rejection).

2.7. fMRI analysis

FMRI data were processed and analyzed using the FSL and AFNI software suites. Within each individual participant, fMRI volumes were co-registered across time to reduce the effects of head motion. Mean fMRI volume of all time points was then computed and co-registered with the T1-weighted structural MRI. Each fMRI volume was smoothed using a Gaussian filter of 4 mm full-width at half maximum. To address motion artifacts, large motion events in the time course, defined as TRs in which there was >0.5 mm of frame-by-frame displacement in the 3-dimension space, were excluded from the analysis. We also excluded the TRs immediately preceding and following the motion-contaminated TRs. All participants included in this study had less than 20% trials excluded. Next, a first-level general linear model of the fMRI data was developed with six motion vectors (three for translation and three for rotation) and one behavioral vector (task) included in deconvolution analysis. The deconvolution analysis did not assume the shape of the hemodynamic response. Instead, the shape of the hemodynamic response function (HRF) was determined by a tent model

estimating each time point independently (0–16 s after the stimulus onset; zero activity was assumed at both ends). The fit coefficients (β-coefficients) represented task-related activity versus baseline at each time point at each voxel. Task-related activity was obtained as summed activity over the expected HRF. Percent signal change was calculated as the ratio of task-related activity against the baseline activity from 2 to 10 s after stimulus onset for reliable HRF estimation in the hippocampus (Stark and Squire 2001).

For the group-level analysis we constructed a sample-specific structural MRI template image using the Advanced Normalization Tools (Avants and Gee 2004). We manually outlined anatomical boundaries of the hippocampus in the structural template image, together with adjacent MTL subregions including perirhinal, entorhinal and parahippocampal cortices (Insausti et al. 1998a; Insausti et al. 1998b). The brain activity map of each individual participant was warped to the structural template space, and resampled to a voxel size of $3 \times 3 \times 3$ mm^3. Consistent with previous studies showing susceptibility-induced signal loss of fMRI in perirhinal and entorhinal cortices (Olman et al. 2009), we identified signal loss in the MTL region. Voxels whose mean fMRI signal intensities were less than half of the global mean intensity of the whole brain were excluded from further analysis. This procedure resulted in exclusion of substantial parts of entorhinal and perirhinal cortices while hippocampus and parahippocampal cortex were well preserved (Fig. 1).

2.8. Hypercapnia image analysis

Data analysis was conducted using the software Statistical Parametric Mapping (SPM2, University College London, UK) and in-house MATLAB (MathWorks, Natick, MA) scripts. Motion correction was performed by realigning all image volumes to the first volume of the scan. Then all the image volumes were smoothed using a Gaussian filter with 8 mm full-width at half maximum. The hypercapnia data were analyzed as a typical block-design fMRI task with one-minute blocks of air vs. gas breathing (Lu et al. 2014). These breathing blocks were temporally aligned with the BOLD fMRI time course data. Then, absolute CVR at each voxel was estimated as percent change of BOLD fMRI signal per mm Hg of EtCO$_2$ change (% BOLD signal/mmHg CO_2). The mean CVR value of the hippocampus for each hemisphere was calculated and used in the analysis.

2.9. Statistical analysis

2.9.1. Task-related fMRI activity

We focused our analyses on ROI-based measures and also used exploratory voxelwise methods. For the ROI-based analyses we used the entire hippocampus in each hemisphere as the anatomical ROI. Mean task-related percent signal change was extracted from the hippocampal ROIs. For the voxelwise analysis, we used two different approaches. In the first approach, we conducted a direct voxelwise search for cluster regions in the MTL where there was an interaction of age by Aβ status on task-related fMRI activity. In the second approach, after identifying cluster regions in the MTL that had significant task-related activity, we examined if there were an interaction of age by Aβ status on the mean task-related fMRI activity in these cluster regions. Statistical maps were first thresholded at a voxelwise p value of 0.05. A cluster-correction technique provided by AFNI was used to correct for multiple comparisons in the MTL mask after censoring for signal loss in fMRI. In this method, Monte Carlo simulations were used to determine how large a cluster of voxels was needed to be statistically meaningful (Forman et al. 1995). The minimum cluster extent was 14 contiguous voxels (378 mm^3) to reach $p < 0.01$ at the cluster level in the MTL mask.

2.9.2. Statistical model

In the main ROI-based analyses as well as the voxelwise analysis, cortical Aβ load status was treated as a categorical variable (Low vs.
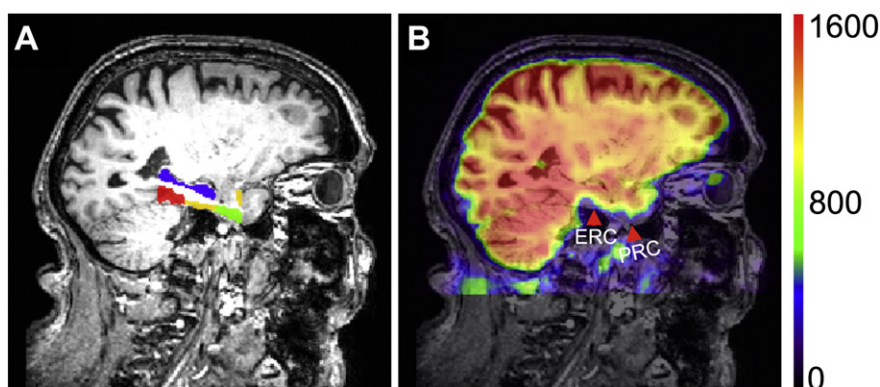
Fig. 1. Signal loss shown for a mean fMRI volume in a representative elderly adult. (A) Anatomical labels of the medial temporal lobe subregions. The definition of labeling colors: blue, hippocampus; green, perirhinal cortex; yellow, entorhinal cortex; red, parahippocampal cortex. (B) The mean fMRI volume of one participant overlaying with 50% transparency on the corresponding MP-RAGE anatomy in the same view as in (A). The two red arrows point to the perirhinal and entorhinal cortices, respectively. The right side color bar indicates intensity of the mean fMRI signals. ERC, entorhinal cortex; PRC, perirhinal cortex.

High) and age as a continuous variable. High Aβ load (Aβ-High) was defined based on the standardized uptake value ratio (SUVr) values of 1.20 or greater. This threshold was chosen based on previous research with the DLBS participants showing that the SUVr of 1.20 was beyond the 95% confidence interval at the age of 60 (Rodrigue et al., 2012), suggesting high cortical Aβ deposition.

To address the issue of data reliability, in two subsequent ROI-based analyses, cortical Aβ load and age were both treated as continuous or both were treated as categorical variables. When age was treated as a categorical variable, the sample was divided at the middle of the entire age range: Age-1 adults were those aged 60–74, and Age-2 adults were aged 75–89. Because there were a disproportionate number of Aβ-Low participants (N = 52) relative to Aβ-High participants (N = 30), we developed an analysis that equated numbers of subjects in each of the four cells in the 2 × 2 ANOVA design, with Age Group and Aβ status as independent variables. The most sparsely populated cell in the full sample analysis was the Age-1/Aβ-High group (N = 13), so we used this as basis for filling the other three cells in an equal number design with 13 subjects per cell. To fill the Age-2/Aβ-High cell, we selected 13 subjects with the highest level of SUVr from this group. We completed the two Aβ-Low cells with participants from the relevant conditions matched to each Aβ-High participant based on age, sex, and education.

3. Results

3.1. ROI-based analysis

We first examined whether cortical Aβ status was associated with task-related activity in the hippocampus. We conducted two separate analyses in the anatomical ROIs of left and right hippocampus, with age treated as a continuous variable and cortical Aβ status as a categorical variable (Low vs. High). In right hippocampus, there were main effects of age ($p = 0.05$) and Aβ status ($p = 0.01$) as well as an interaction of age by Aβ status ($p = 0.02$). As displayed in Fig. 2, the interaction was significant because Aβ-Low participants exhibited a significant age-related decrease in hippocampal activity ($p = 0.03$, $R^2 = 0.09$), whereas Aβ-High participants displayed no significant age-related difference in hippocampal activity ($p = 0.23$, $R^2 = 0.05$). In the left hippocampus, we found no main effect of Aβ status or age ($p > 0.35$) nor an interaction ($p = 0.53$). We also included sex as a covariate, but the findings remained unchanged for both the left and right hippocampus. Finally, we note that after applying a Bonferroni correction to the main general linear analyses conducted in left and right hippocampi, the main effect of Aβ status and the interaction of age by Aβ status remained significant in right hippocampus ($p < 0.05$).

To explore the reliability of the interaction in the right hippocampus, we conducted several variations of the main analysis. First we treated both age and cortical Aβ load as continuous variables, and found a main effect of cortical Aβ load ($p = 0.05$), a marginal effect of age ($p = 0.08$), as well as a marginal interaction ($p = 0.09$). Next we treated both age and cortical Aβ load as categorical variables in a 2 × 2 ANOVA, i.e. Age Group (Age-1 vs. Age-2) and Aβ status (Low vs. High). There was a marginal main effect of Age Group ($F = 3.44$, $p = 0.07$), a main effect of Aβ status ($F = 5.43$, $p = 0.02$), and a marginal interaction ($F = 3.60$, $p = 0.06$). We also conducted this categorical analysis with the matched sample (13 participants per cell, described in Methods). As shown in Fig. 3, we found a marginally significant effect of Age Group ($F = 2.63$, $p = 0.11$), a significant main effect of Aβ status ($F = 5.28$, $p = 0.03$), and a marginal interaction ($F = 2.93$, $p = 0.09$). We note that all the observed interactions were of the same form as depicted in Figs. 2 and 3.
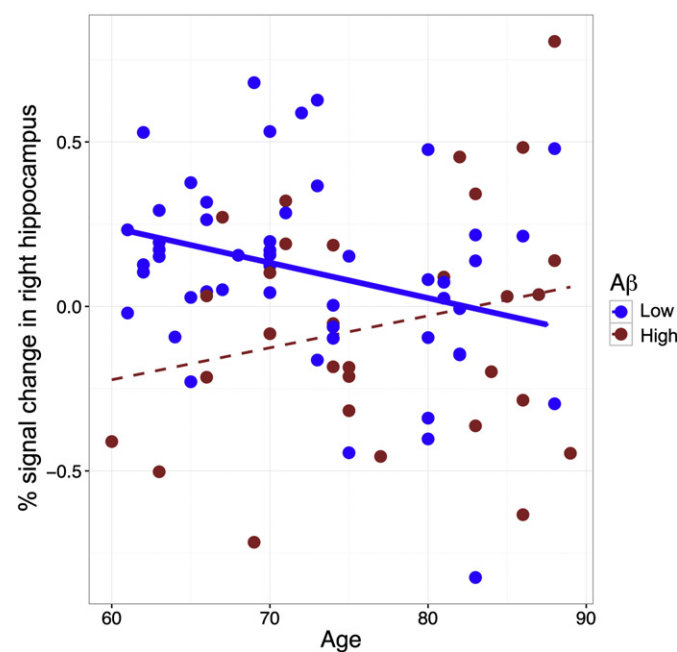

Fig. 2. The interaction of age by cortical Aβ status (Low vs. High) on the mean task-related fMRI signal change of the entire right hippocampus ($p = 0.02$). The dashed fitting line for the Aβ-High group indicates a trend ($p > 0.20$).
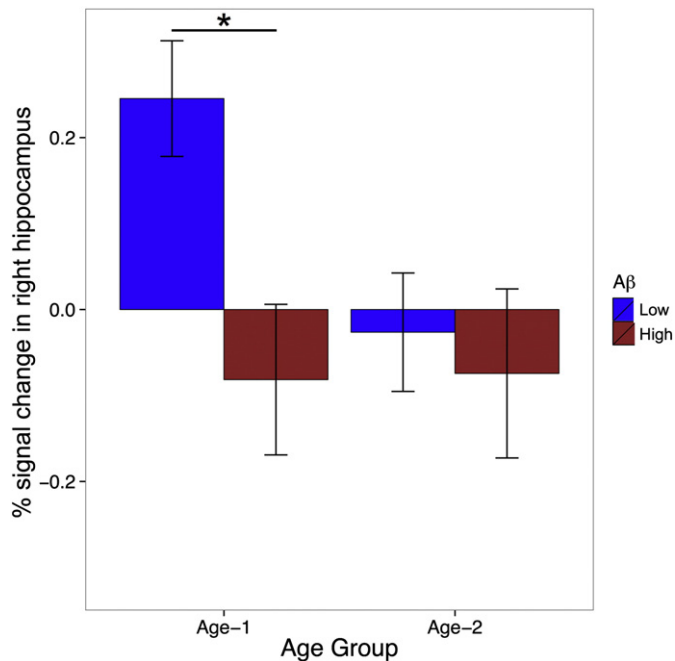
Fig. 3. In a matched subsample (N = 52), the effect of cortical Aβ status (Low vs. High) and Age Group (Age-1: 60–74; Age-2: 75–89) on task-related fMRI signal change of the entire right hippocampus when both variables were treated as category variables. There was a main effect of Aβ status ($p = 0.03$). The interaction of Age Group by Aβ status was approaching to significance ($p = 0.09$). There was greater activation in the Aβ-Low than Aβ-High participants in the younger Age-1 group ($p = 0.007$) but not in the older Age-2 group. Error bars indicate standard errors.

3.1.1. Episodic memory

We examined accuracy of episodic memory performance on the incidental memory-encoding task performed in the scanner and also analyzed general episodic memory function collected as part of the cognitive battery outside of the scanner. A general linear model on subsequent recognition accuracy for which age was treated as a continuous variable and cortical Aβ status as a categorical variable yielded only a main effect of age ($p = 0.0001$). We repeated the same general linear analysis on the episodic memory construct score derived from the cognitive battery, which yielded no main effects of Aβ status or age, nor an interaction. In a second set of analyses, we repeated the main general linear analysis on right hippocampal activity, controlling for either subsequent recognition accuracy of the fMRI task or the general episodic memory construct score. Results indicated no change in the original finding of the main effect of Aβ status and its interaction with age, confirming that the Aβ effect and its interaction with age on the task-related hippocampal activity was not compromised by either task-specific or general episodic memory performance.

3.1.2. Cerebrovascular reactivity

We examined whether neurovascular coupling, measured as CVR, might affect the Aβ effects on task-related hippocampal activity. A subset of participants in the present study (N = 50, 16 Aβ-High/34 Aβ-Low) underwent hypercapnia MRI that measured CVR in the brain (Table 1). We note that of the 16 Aβ-High, 9 were in the Age-1 group and 7 in the Age-2 group. These numbers were insufficient to execute our plan to first detect the interaction of age by Aβ status in the general linear analysis, and then examine whether the interaction was compromised by regional CVR. As an alternative, we conducted t-tests that compared the effect of Aβ status (High vs. Low) in the Age-1 and Age-2 groups respectively. In the right hippocampus, as we predicted, the difference between Aβ-High and Aβ-Low participants in the Age-1 group within this hypercapnia subset approached significance ($p =$

0.07). Interestingly, when we added regional CVR as a covariate, the effect of Aβ status became significant ($p = 0.04$), suggesting a small role for CVR in modulating the effects. Also, consistent with the main finding, there was no significant effect of Aβ status in the Age-2 participants within this hypercapnia subset ($p = 0.72$), and the effect remained nonsignificant after controlling for regional CVR ($p = 0.88$). No effects were observed in the left hippocampus. To summarize, the observed effects were consistent with the original sample, suggesting that regional CVR played a limited role in modifying our original findings. We do, however, recognize that power is limited and a larger sample is needed to confirm this finding.

3.2. Voxelwise analysis

In a more exploratory vein, we broadened our analyses to encompass the entire MTL. This allowed us to assess whether the interaction observed in the right hippocampus was specific to that region or could be found elsewhere in the MTL. In the first approach, a voxelwise search yielded no cluster regions in the MTL for neither a main effect of Aβ status nor an interaction of age by Aβ status. In the second approach, we identified two target cluster regions in the MTL that had significant task-related activity in the Age-1/Aβ-Low group (see Fig. 4), essentially treating this group as a control condition, and then examined these regions in the entire sample for an interaction of age by Aβ status. One cluster region was located mainly in right parahippocampal cortex (2970 mm^3). A substantial part of the body of right hippocampus was included in this cluster (432 mm^3), the size of which was already larger than the clustering threshold. The second cluster was located mainly in left parahippocampal cortex (3564 mm^3). When we examined the interaction of age by Aβ status in the two clusters for the entire sample (N = 82), we found no evidence for either the two main effects or the interaction ($p > 0.50$). However, when we extracted mean percent signal change from the portion of right hippocampus within the cluster in the right MTL, there was a main effect of Aβ status ($p = 0.05$) and a marginal interaction of age by Aβ status ($p = 0.09$), but no main effect of age ($p = 0.22$). These findings were comparable to the ROI-based analysis of the entire right hippocampus (Fig. 2).

4. Discussion

The major findings from the present study are as follows. First, in the cognitively normal elderly, task-related hippocampal activity was associated with cortical Aβ status, which interacted with advancing age. Specifically, the younger elderly with low cortical Aβ showed more task-related activation in right hippocampus than those with high cortical Aβ load. However, the observed difference was less evident with advancing age. Second, the Aβ effect and its interaction with age on hippocampal activity remained the same after controlling for task-specific memory performance and a general episodic memory score. Furthermore, in a subset of participants with hypercapnia MRI, controlling for regional CVR, which has been hypothesized to be a potential modifying factor of fMRI signals (Liu et al. 2013), had little effect on the results. Finally, there were no effects associated with Aβ in either the left hippocampus or the parahippocampal gyrus. There are two possible reasons for the null findings in these MTL regions. First, the task-related activity in these regions may depend on the specific task. Our data do not rule out the possibilities that other memory-related fMRI tasks might identify Aβ effects in the left hippocampus or other MTL regions. Second, fMRI signal loss, which is quite typical, made it difficult to detect subtle effects on task-related activity in entorhinal and perirhinal cortices (see Fig. 1), the MTL regions where tau pathology may develop at the earliest stage of AD and thus are highly likely related to cortical Aβ deposition (Khan et al. 2014).

The present study also provides evidence that task-related hippocampal activity is generally weak in cognitively-normal elderly with either high cortical Aβ load or of very old age, and that Aβ status serves
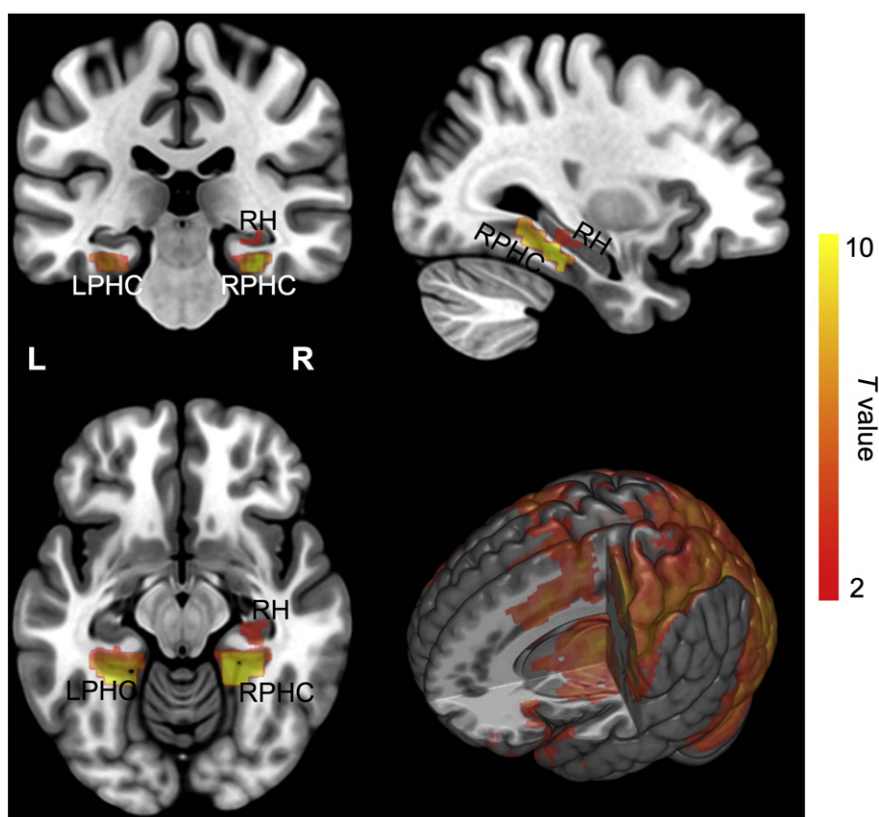
Fig. 4. *T*-maps of identified cluster regions in the medial temporal lobe that assessed fMRI signal change during the incidental memory-encoding task compared with the fixation baseline in the younger Age-1 group (aged 60–74) who had low cortical Aβ load. The *t*-map of the whole brain is also displayed in a rendered 3D image, in which part of right hemisphere is removed to expose deep brain structures. The *t*-maps are displayed with MRIcroGL after warping from the sample-specific template to the MNI-152 template, being thresholded at $t = 2.0$ that corresponds with $p = 0.05$ at the voxel level. The color bar indicates *t*-value. RH, right hippocampus; RPHC, right parahippocampal cortex; L, left; R, right.

as a proxy for tau accumulation across the MTL. It may seem paradoxical that high cortical Aβ load was associated with low task-related hippocampal activity in the younger elderly. This finding, however, does not preclude the possibility that the high Aβ participants actually had neural hyperactivity in the hippocampal region. If high Aβ participants consistently exhibited neural hyperactivity in the hippocampus across both task and baseline conditions, then the contrast of task versus baseline inherent to the present design might yield a low value. This finding is compatible with a previous finding that high Aβ was related to a smaller activity difference between task and baseline in the entorhinal cortex (Huijbers et al. 2014). The issue could be further illuminated by the use of metabolism imaging methods (e.g. FDG-PET) in future studies.

Based on these findings, we conclude that cortical Aβ deposition exerts an effect on task-related hippocampal activity in early, but not later, old age in cognitively-normal adults. This result may provide an explanation for the previous mixed findings regarding the Aβ effect on hippocampal activity in cognitively-normal older adults. Of the few studies that have addressed the relationship between Aβ and hippocampal activity in the cognitively-normal elderly, all had a high mean age for participants, ranging from 75.4 to 76.4 (Sperling et al. 2009; Mormino et al. 2012; Elman et al. 2014; Huijbers et al. 2014). The present result suggests the possibility that the reported null effects in many of these studies might be due to the inclusion of a disproportionate number of very old adults. There is a large literature showing that with advanced age, neural signals are increasingly less selective and "dedifferentiated" across many domains (Park et al. 2004; Carp et al. 2011), and the lack of a specific neural signature in older adults likely represents another instantiation of this general finding.

One issue, with respect to the present finding, may be why cortical Aβ deposition should be found to be associated with hippocampal activity in the MTL. We suggest that a high level of amyloid deposition across

the neocortex may serve as a proxy for tau pathology in the MTL. These two pathologies originate in separate brain regions and follow different routes of spreading (Braak et al. 2011). However, there is increasing evidence from both postmortem and imaging studies that the development of these two pathologies is highly correlated (Braak et al. 2011; Sperling et al. 2014). Besides the development of tau pathology, soluble Aβ peptides may also present in the MTL in early AD (Small 2014). Soluble Aβ peptides are not measurable by either imaging or histological methods, yet they appear to be highly neurotoxic (Mucke and Selkoe 2012).

It is important to note that both Aβ and tau pathologies are associated with aberrant neural hyperactivity (Small 2014), which has been observed at different phases of AD and which eventually leads to neuronal cell death (Palop and Mucke 2009). This idea is compatible with the notion that tau pathology in the MTL, which is indicated by high Aβ load in the neocortex, may result in disruption of hippocampal activity. Consistent with this view, high cortical Aβ load has been associated with low resting-state fMRI connectivity between the hippocampus and perirhinal cortex in the cognitively-normal elderly (Song et al. 2015). The perirhinal cortex is vulnerable to tau pathology in the earliest stage of AD (Braak and Braak 1991) and is closely connected with the hippocampus.

We note that aging itself, even in the absence of Aβ, is a complex process that may alter hippocampal activity, making it more challenging to identify the effect of AD-related pathologies in this region. For example, in two similar cross-sectional subsequent memory studies, one reported that older age was related to lower task-related hippocampal activity in memory encoding tasks (Gutchess et al. 2005) while the other reported no age effect (Morcom et al. 2007). More recently, a longitudinal fMRI study of middle and old age (aged 55–79) found age-related reduction of task-related hippocampal activity in a

memory-encoding task, and the reduction was positively related to memory decline (Persson et al. 2012). The longitudinal data represent convincing evidence that hippocampal activity does decline with advanced age, adding credence to the present results and the likelihood that reductions in hippocampal activity occur continuously with advancing age. To our best knowledge, however, there have been no studies showing how age alters hippocampal activity within older populations (e.g. 60 and older). Overall, the corpus of existing data indicates that interactions with age are important to take into account in analysis of the effect of AD-related pathologies on hippocampal activity.

One other challenge of the present study was associated with measurement of MTL activity in fMRI experiments. Data collection with fMRI in the MTL region is vulnerable to severe susceptibility-induced signal loss (Olman et al. 2009), particularly in the entorhinal and perirhinal areas because of their adjacency to air-tissue boundaries (Fig. 1). This intrinsic difficulty of fMRI prevents reliable measurements in these regions, while they are of great interest in the studies of early AD (Braak and Braak 1991). This methodological limitation precluded accurate assessment of these MTL regions other than hippocampus in the present study.

5. Conclusion

We found that high cortical Aβ load in cognitively-normal elderly was related to weaker task-related hippocampal activity in an incidental memory encoding task. Importantly, there was an interaction between cortical Aβ load and age so that the Aβ effect on hippocampal activity was found more evident in a younger age. The finding was maintained even after taking into account subsequent memory performance of the fMRI task and a general episodic memory score. Given the strong connectivity between the hippocampus and adjacent MTL structures, the association between cortical Aβ load and hippocampal activity is indicative of functional alteration in the hippocampus-centered memory network in the MTL, which is also vulnerable to tau pathology in the earliest phase of AD.

Acknowledgement

References

Avants, B., Gee, J.C., 2004. Geodesic estimation for large deformation anatomical shape averaging and interpolation. NeuroImage 23 (Suppl. 1), S139–S150.

Braak, H., Braak, E., 1991. Neuropathological stageing of Alzheimer-related changes. Acta Neuropathol. 82, 239–259.

Braak, H., Thal, D.R., Ghebremedhin, E., Del Tredici, K., 2011. Stages of the pathologic process in Alzheimer disease: age categories from 1 to 100 years. J. Neuropathol. Exp. Neurol. 70, 960–969.

Brandt, J., 1991. The Hopkins verbal learning test: development of a new memory test with six equivalent forms. Clin. Neuropsychol. 5, 125–142.

Carp, J., Park, J., Hebrank, A., Park, D.C., Polk, T.A., 2011. Age-related neural dedifferentiation in the motor system. PLoS One 6, e29411.

D'Esposito, M., Deouell, L.Y., Gazzaley, A., 2003. Alterations in the BOLD fMRI signal with ageing and disease: a challenge for neuroimaging. Nat. Rev. Neurosci. 4, 863–872.

Ekstrom, R.B., French, J.W., Harman, H., Derman, D., 1976. Kit of Factor-Referenced Cognitive Tests. Rev. ed. Educational Testing Service, Princeton, NJ.

Elman, J.A., Oh, H., Madison, C.M., Baker, S.L., Vogel, J.W., Marks, S.M., Crowley, S., O'Neil, J.P., Jagust, W.J., 2014. Neural compensation in older people with brain amyloid-beta deposition. Nat. Neurosci. 17, 1316–1318.

Forman, S.D., Cohen, J.D., Fitzgerald, M., Eddy, W.F., Mintun, M.A., Noll, D.C., 1995. Improved assessment of significant activation in functional magnetic resonance imaging (fMRI): use of a cluster-size threshold. Magn. Reson. Med. 33, 636–647.

Gutchess, A.H., Welsh, R.C., Hedden, T., Bangert, A., Minear, M., Liu, L.L., Park, D.C., 2005. Aging and the neural correlates of successful picture encoding: frontal activations compensate for decreased medial-temporal activity. J. Cogn. Neurosci. 17, 84–96.

Huijbers, W., Mormino, E.C., Wigman, S.E., Ward, A.M., Vannini, P., McLaren, D.G., Becker, J.A., Schultz, A.P., Hedden, T., Johnson, K.A., Sperling, R.A., 2014. Amyloid deposition is linked to aberrant entorhinal activity among cognitively normal older adults. J. Neurosci. 34, 5200–5210.

Insausti, R., Insausti, A.M., Sobreviela, M.T., Salinas, A., Martinez-Penuela, J.M., 1998a. Human medial temporal lobe in aging: anatomical basis of memory preservation. Microsc. Res. Tech. 43, 8–15.

Insausti, R., Juottonen, K., Soininen, H., Insausti, A.M., Partanen, K., Vainio, P., Laakso, M.P., Pitkanen, A., 1998b. MR volumetric analysis of the human entorhinal, perirhinal, and temporopolar cortices. AJNR Am. J. Neuroradiol. 19, 659–671.

Jack Jr., C.R., Holtzman, D.M., 2013. Biomarker modeling of Alzheimer's disease. Neuron 80, 1347–1358.

Kennedy, K.M., Rodrigue, K.M., Devous Sr., M.D., Hebrank, A.C., Bischof, G.N., Park, D.C., 2012. Effects of beta-amyloid accumulation on neural function during encoding across the adult lifespan. NeuroImage 62, 1–8.

Khan, U.A., Liu, L., Provenzano, F.A., Berman, D.E., Profaci, C.P., Sloan, R., Mayeux, R., Duff, K.E., Small, S.A., 2014. Molecular drivers and cortical spread of lateral entorhinal cortex dysfunction in preclinical Alzheimer's disease. Nat. Neurosci. 17, 304–311.

Liu, P., Hebrank, A.C., Rodrigue, K.M., Kennedy, K.M., Section, J., Park, D.C., Lu, H., 2013. Age-related differences in memory-encoding fMRI responses after accounting for decline in vascular reactivity. NeuroImage 78, 415–425.

Lu, H., Liu, P., Yezhuvath, U., Cheng, Y., Marshall, O., Ge, Y., 2014. MRI Mapping of Cerebrovascular Reactivity via Gas Inhalation Challenges (Journal of visualized experiments).

Morcom, A.M., Li, J., Rugg, M.D., 2007. Age effects on the neural correlates of episodic retrieval: increased cortical recruitment with matched performance. Cereb. Cortex 17, 2491–2506.

Mormino, E.C., Brandel, M.G., Madison, C.M., Marks, S., Baker, S.L., Jagust, W.J., 2012. A beta deposition in aging is associated with increases in brain activation during successful memory encoding. Cereb. Cortex 22, 1813–1823.

Mucke, L., Selkoe, D.J., 2012. Neurotoxicity of amyloid beta-protein: synaptic and network dysfunction. Cold Spring Harb. Perspect. Med. 2, a006338.

Olman, C.A., Davachi, L., Inati, S., 2009. Distortion and signal loss in medial temporal lobe. PLoS One 4, e8160.

Palop, J.J., Mucke, L., 2009. Epilepsy and cognitive impairments in Alzheimer disease. Arch. Neurol. 66, 435–440.

Park, D.C., Polk, T.A., Park, R., Minear, M., Savage, A., Smith, M.R., 2004. Aging reduces neural specialization in ventral visual cortex. Proc. Natl. Acad. Sci. U. S. A. 101, 13091–13095.

Persson, J., Pudas, S., Lind, J., Kauppi, K., Nilsson, L.G., Nyberg, L., 2012. Longitudinal structure-function correlates in elderly reveal MTL dysfunction with cognitive decline. Cereb. Cortex 22, 2297–2304.

Raven, J., Raven, J.C., Court, J.H., 1998. Manual for Raven's Progressive Matrices and Vocabulary Scale. The Psychological Corporation, San Antonio, TX.

Robbins, T.W., James, M., Owen, A.M., Sahakian, B.J., McInnes, L., Rabbitt, P., 1994. Cambridge Neuropsychological Test Automated Battery (CANTAB): a factor analytic study of a large sample of normal elderly volunteers. Dementia 5, 266–281.

Rodrigue, K.M., Kennedy, K.M., Devous Sr., M.D., Rieck, J.R., Hebrank, A.C., Diaz-Arrastia, R., Mathews, D., Park, D.C., 2012. beta-Amyloid burden in healthy aging: regional distribution and cognitive consequences. Neurology 78, 387–395.

Salthouse, T.A., Babcock, R.L., 1991. Decomposing adult age differences in working memory. Dev. Psychol. 27, 763–776.

Small, S.A., 2014. Isolating pathogenic mechanisms embedded within the hippocampal circuit through regional vulnerability. Neuron 84, 32–39.

Song, Z., Insel, P.S., Buckley, S., Yohannes, S., Mezher, A., Simonson, A., Wilkins, S., Tosun, D., Mueller, S., Kramer, J.H., Miller, B.L., Weiner, M.W., 2015. Brain amyloid-beta burden is associated with disruption of intrinsic functional connectivity within the medial temporal lobe in cognitively normal elderly. J. Neurosci. 35, 3240–3247.

Sperling, R.A., Laviolette, P.S., O'Keefe, K., O'Brien, J., Rentz, D.M., Pihlajamaki, M., Marshall, G., Hyman, B.T., Selkoe, D.J., Hedden, T., Buckner, R.L., Becker, J.A., Johnson, K.A., 2009. Amyloid deposition is associated with impaired default network function in older persons without dementia. Neuron 63, 178–188.

Sperling, R.A., et al., 2011. Toward defining the preclinical stages of Alzheimer's disease: recommendations from the National Institute on Aging-Alzheimer's Association workgroups on diagnostic guidelines for Alzheimer's disease. Alzheimers Dement. 7, 280–292.

Sperling, R., Mormino, E., Johnson, K., 2014. The evolution of preclinical Alzheimer's disease: implications for prevention trials. Neuron 84, 608–622.

Stark, C.E., Squire, L.R., 2001. When zero is not zero: the problem of ambiguous baseline conditions in fMRI. Proc. Natl. Acad. Sci. U. S. A. 98, 12760–12766.

Turner, M.L., Engle, R.W., 1989. Is working memory capacity task dependent? J. Mem. Lang. 28, 127–154.

Wechsler, D., 1997. Wechsler Adult Intelligence Scale–III (WAIS-III). Psychological Corporation, New York.

Zachary, A.S.W.C., 1986. Shipley Institute of Living Scale. Revised Manual.Western Psychological Services, Los Angeles.